



Fermi National Accelerator Laboratory

FERMILAB-Conf-82/69-EXP
7550.537
7184.326

DIMUON PRODUCTION IN HADRONIC INTERACTIONS*

B. Cox

October 1982

*Rapporteur Talk XXI International Conference on High Energy Physics, Paris, France, July 26-31, 1982.



DIMUON PRODUCTION IN HADRONIC INTERACTIONS

B. Cox

Fermi National Accelerator Laboratory

Rapporteur Talk

XXI International Conference on High Energy Physics
Paris, France

Abstract

This report summarizes the new data submitted to the XXI International Conference on High Energy Physics on high mass dimuon production in π^-N and $\bar{p}N$ interactions by Fermilab Experiment E-537, CERN Experiment NA3 and Fermilab Experiment E-326. Successes and failures of the Drell-Yan model and low order QCD are reviewed. New results on the production of the J/ψ from E-537, NA3 and CERN experiment WA11 are also reported.

Introduction - Experiments which measure the production of high mass ($M > 4 \text{ GeV}/c^2$) dilepton pairs present opportunities to confront the constituent picture of hadrons which has evolved in the last decade. Comparison of the dilepton data with the predictions of the Drell-Yan model¹ (zeroth order QCD) and the Compton and annihilation processes² (first order QCD) allow the quark and gluon structure of the hadrons to be determined. Studies of the production of lepton pairs in $\bar{p}N$ collisions provide an opportunity to test the Drell-Yan and QCD picture of hadronic production of lepton pairs using the nucleon structure functions determined in deep inelastic lepton scattering experiments. Measurements of high mass lepton pair production in πN interactions make it possible to measure pion structure functions which cannot be determined in deep inelastic lepton scattering experiments. New data has been presented at this conference on the production of high mass lepton pairs in both $\bar{p}N$ and π^-N interactions.^{3,4,5}

In addition to the new data on the high mass lepton pair production new data has been reported at this conference on the production of $J/\psi(3.1)$ in $\bar{p}N$ and π^-N interactions.⁶⁻⁸ In the same manner that high mass pair production sheds light on hadronic quark structure functions, the measurement of direct J/ψ production has been used to determine gluon structure functions.⁷ Finally the observation of multiple ψ production has been reported.⁸ The production of di- ψ events may be an indication of rare processes such as $\bar{B}B$ production.

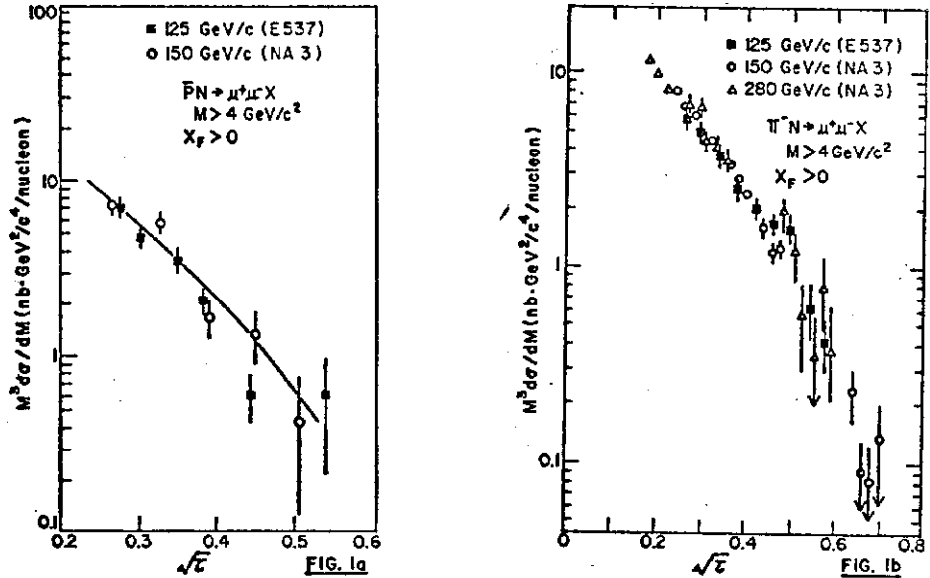
High Mass Muon Pair Production - The confrontation of Drell-Yan and first order QCD with the high mass muon pair production data has had both successes and failures to date. The inability of the naive Drell-Yan model to predict the absolute level of the cross sections for μ pair production has been quantified as the 'K factor' for πN and $\bar{p}N$ reactions. This quantity is defined as the ratio of the measured cross section to the Drell-Yan prediction (using some choice of hadronic structure functions such as the CDHS nucleon structure functions). The preliminary new results (denoted by the asterisks) from E-537 for K are shown in Table 1 along with the results of previous experiments.

Table 1: Experimental K Factors ($K = \frac{d\sigma}{dM dX_F} \text{ data} / \frac{d\sigma}{dM dX_F} \text{ Drell-Yan}$)

P _{Lab}	Beam/Target	K	Experiment
* 125	$\bar{p}N$	2.25 ± 0.45	Fermilab E-537
150	pN	2.3 ± 0.4	CERN NA3
39.5	π^+N	2.6 ± 0.5	CERN BCE (Omega)
* 125	π^-N	2.5 ± 0.5	Fermilab
150,200	π^-N	2.2 ± 0.3	CERN NA3
150	π^+N	2.4 ± 0.4	CERN NA3
150	π^-p	2.4 ± 0.4	CERN NA3
150,175	π^-p	2.8	CERN WA11
150	pN	2.2 ± 0.4	CERN NA3
400	pN	1.7	Fermilab E-288
400	pN	1.6 ± 0.3	Fermilab E-439
2115 ($\sqrt{s}=63$)	pp	1.6	CERN R-209

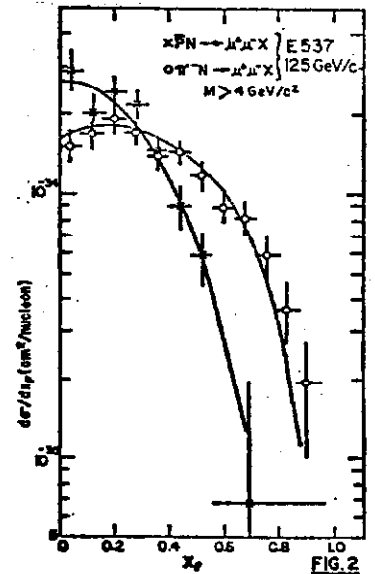
The data given in Table 1 for πN reaction are consistent with one another but the pN data show three experiments with K factors of approximately 1.6 to 1.7 and one experiment, NA3 with a nucleon K factor of 2.2. The new $\bar{p}N$ data shown by E-537 is the only other experiment besides the NA3 experiment to obtain a K factor greater than 2 for the nucleon or antinucleon reactions. Other than the problem with the nucleon K factors the data seem consistent with a K factor relatively independent of beam type and in general greater than two. No experimental evidence has yet been presented that would suggest that the K factor is a function of any kinematic variable.

Using Proton West enriched antiproton beam (obtained from $\bar{\Lambda} \rightarrow \bar{p}\pi^+$ decays) Fermilab Experiment E-537 recently completed the highest statistics measurement of $\bar{p}N \rightarrow \mu^+\mu^-$ to date.



The scaling cross section, $M^3 d\sigma/dM$, determined by the E-537 experimenters is shown in Fig. 1a along with the higher energy NA3 $\bar{p}N$ data. The solid line is 2.3 times the simple Drell-Yan calculation of this cross section obtained by using the CDHS structure functions.⁹ Figure 1b shows new data from E-537 for $\pi^-N \rightarrow \mu^+\mu^-X$ along with older data from NA3 at other energies. These figures indicate two of the successes of the simple Drell-Yan model (prediction of the shape of $M^3 d\sigma/dM$ and the scaling property of this cross section) and one of the failures (inability to predict the absolute level of the cross section).

A third success of simple Drell-Yan has been the prediction of the shape of the X_F distribution for dimuon production. In particular, as seen from the E-537 data shown in Fig. 2, shape of the X_F distribution (but once again, not the absolute level) is well predicted for $\bar{p}N \rightarrow \mu^+\mu^-X$ using the CDHS structure functions. This reaction 'tests' the Drell-Yan picture more completely than the π^-N dimuon data as a function of X_F must be used to extract the pion structure function. In the case of the $\bar{p}N$ reaction the nucleon structure functions can be obtained independently from deep inelastic lepton scattering. The curves in Fig. 2 are the naive Drell-Yan prediction using CDHS structure functions for the $\bar{p}N$ reaction and NA3 pion structure functions for the π^-N data. These predictions are multiplied by the E-537 K factors given in Table 1. These data indicate that the structure functions for the \bar{p} and π^- are roughly



consistent with CDHS and NA3 structure functions respectively. The E-537 experimenters have not yet made an independent determination of structure functions from their data.

Fermilab experiment E-326 has made the independent determination of the pion valence structure function as shown in Fig. 3 using a part of their 225 GeV/c π^-N data. After checking that the factorization of $M^4 d\sigma/dX_1 dX_2$ into a product of a function of X_1 and a function of X_2 is valid, the E-326 experimenters have extracted the pion structure function $V_\pi(X_1) = (0.75 \pm 0.2)\sqrt{X}(1-X)^{1.01 \pm 0.10}$

which is consistent with previous NA3 measurement. At the current stage of their analysis, they have used the pion sea quark distributions of NA3 rather than independently determining the sea distribution from their data.

The analysis of the dimuon cross sections as a function of \sqrt{s} and X_F that have been reported above in general depend only on the simple Drell-Yan picture with little or no need for recourse to higher order QCD. However, when the p_T spectrum of the dimuon is analyzed, QCD effects appear. Higher order processes in α_s such as gluon Compton scattering or quark-antiquark annihilation contribute and produce high p_T muon pairs. Two different techniques have been used in the contributions to the conference to analyze the p_T of the dimuon system. E-537 has analyzed the shape of the p_T distributions of their 125 GeV/c \bar{p} and π^- data (shown in Fig. 4) by the Altarelli, Parisi, and Petronzio technique.¹⁰ The nongaussian tail of the p_T distribution is explained in this technique by the Compton and annihilation processes. An intrinsic $\langle k_T^2 \rangle \sim 0.88 \text{ GeV}^2/c^2$ (which has been observed in $pN \rightarrow \mu^+\mu^-$ interactions¹¹), counting rule gluon structure functions and NA3 and CDHS quark structure functions have been used to produce the curves which are shown in Fig. 4. However, this technique requires the assumption that the hard gluon processes are the only contributors to the high p_T tail. In fact, soft gluon processes may very well contribute and the $\langle k_T^2 \rangle$ which is needed to explain the data may be an overestimate.

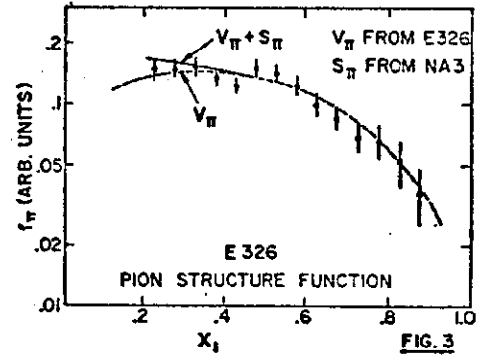


FIG. 3

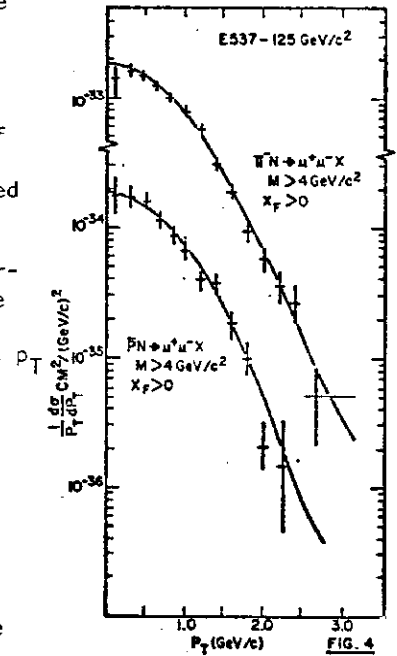


FIG. 4

A second method can be used to determine the intrinsic k_T of the constituents if the S dependence of $\langle p_T^2 \rangle$ is assumed to be due to QCD processes. Then a linear extrapolation of $\langle p_T^2 \rangle$ (but not necessarily $\langle p_T \rangle$) to $S=0$ should yield an 'intrinsic' $\langle k_T^2 \rangle$. Figure 5 shows $\langle p_T^2 \rangle$ vs. S for several $\pi^-N \rightarrow \mu^+\mu^-$ measurements. NA3 have fitted their three data points at 150, 200 and 280 GeV/c to a linear form, $\langle p_T^2 \rangle = A + BS$. They find $\langle p_T^2 \rangle = (0.76 \pm 0.07) + (0.0025 \pm 0.0002)S \text{ GeV}^2/c^2$. If all the data in the plot including the new E-537 point are fit, $\langle p_T^2 \rangle = (0.62 \pm 0.05) + (0.0028 \pm 0.0002)S$ is obtained. This second fit is shown in Fig. 5. Figure 6 shows a similar plot of $\langle p_T^2 \rangle$ vs. S prepared for $pN \rightarrow \mu^+\mu^-$. The proton data when fit with $\langle p_T^2 \rangle = A + BS$ yields $\langle p_T^2 \rangle = (0.59 \pm 0.19) + (0.0013 \pm 0.0002)S$. The slope is less than that observed in Fig. 5, but the intercept which we are defining to be intrinsic k_T

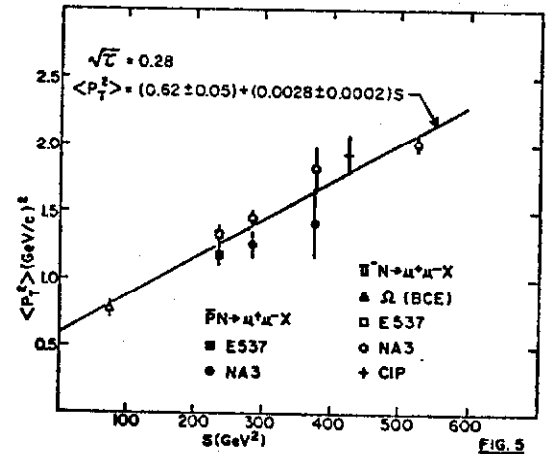


FIG. 5

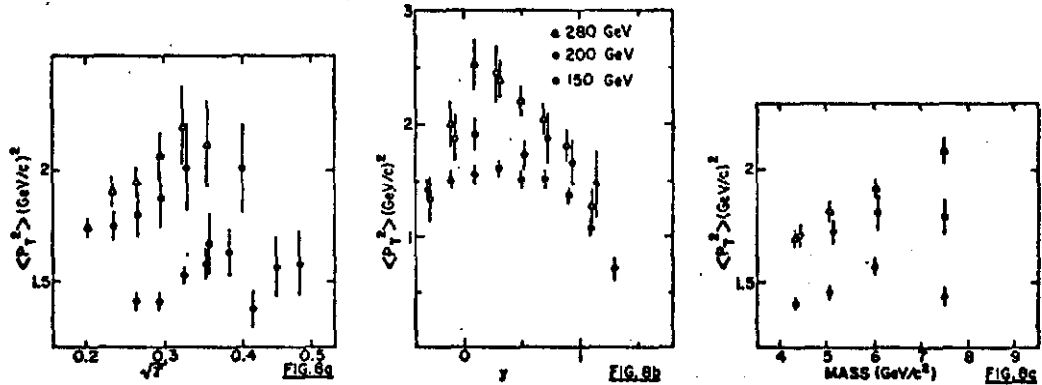
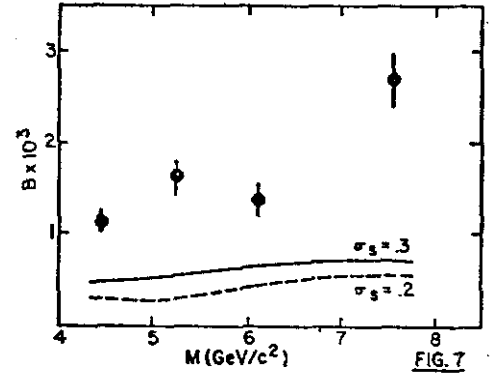
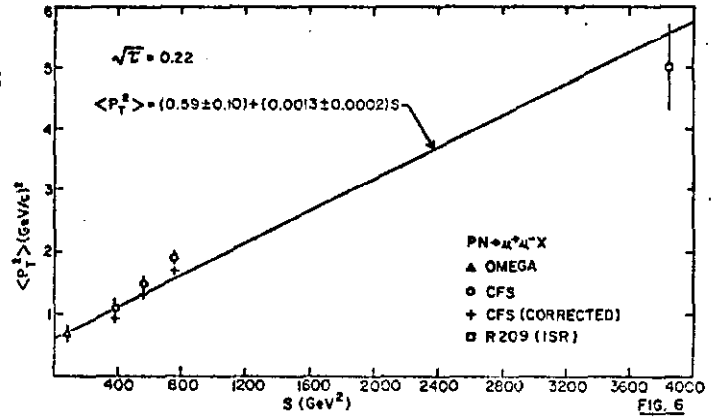
is approximately the same for the proton and pion data. (The three E-288 data points have been lowered slightly to account for the fact that they are $X_F=0$ data. The average of all events at $X_F > 0$ is expected by the Altarelli model to have a 15% lower $\langle p_T^2 \rangle$ than the $X_F = 0$ data.) In addition the $\bar{p}N$ data (see Fig. 5) from E-537 and NA3 while not of the quality of the π^-N data seem to be similar to the pion measurements except that the $\langle p_T^2 \rangle$ for the \bar{p} data is slightly lower at a given energy. Part of the difference in slope of the S dependence may be due to the different S dependence of valence-valence quark interactions (which dominate $\bar{p}N$ and π^-N reactions) and valence-sea quark interactions (which dominate pN interactions). The observation of similar intercepts of these two plots suggests similar intrinsic k_T for valence and sea quarks in protons and pions.

The NA3 experimenters have attempted to predict the slope of their π^-N data (Fig. 5) due to the annihilation and Compton processes. The expected $\langle p_T^2 \rangle$ is given by

$$\langle p_T^2 \rangle = \frac{L \int dp_T^2 \left[\frac{d\sigma_A}{dp_T^2} + \frac{d\sigma_C}{dp_T^2} \right] p_T^2}{K \sigma_0}$$

where σ_A , σ_C , and σ_0 are the annihilation, Compton, and Drell-Yan cross sections respectively. K is the K factor previously defined and L is a corrective multiplier which is used to parameterize the discrepancy between the predicted and observed $\langle p_T^2 \rangle$. As can be seen from Fig. 7, the calculation (for $L=1, K=1.8$) of the slope $\langle p_T^2 \rangle$ vs. S falls far short of the observed slope at different masses. For $\alpha_S = 0.3$, $L/K = 1.52 \pm 0.13$ and L/K is increasing with M :

The NA3 experimenters have also displayed $\langle p_T^2 \rangle$ as a function of \sqrt{T} , y , and mass at each of their three energies. As seen in Fig. 8a, b, c there are strong variations of $\langle p_T^2 \rangle$ with each of these variables and in general the strength of the variation increases with energy. Explanation of this data by quantum chromodynamics will be a challenge for the future.



Production of the J/ψ Resonance - Three new contributions on the production of J/ψ resonance have been reported at this conference by the E-537,⁶ NA3⁷ and WA11⁸ experimenters. E-537 has studied the antiproton production of J/ψ at 125 GeV/c and in particular emphasized the comparison of these cross sections with π^-N production of J/ψ at the same energy. The ratio of total cross sections ($\sigma_{\bar{p}}/\sigma_{\pi^-} = 0.88 \pm 0.05$) shown in Fig. 9a requires a large gluon fusion contribution to J/ψ production according to the gluon/quark fusion model of Barger, et al.,¹² to equalize the \bar{p} and π^- cross sections. The ratio $\sigma_{\bar{p}}/\sigma_{\pi^-}$ shown in Fig. 9b indicates that gluon fusion is the most important contribution to J/ψ production in nucleon-nucleon interactions at high energies, and is needed to explain the energy dependence of the $\sigma_{\bar{p}}/\sigma_{\pi^-}$ ratio. The dotted curve in Fig. 9b is the prediction of the χ production model⁹ of Carlson and Suaya¹³ in which the J/ψ 's are produced through an intermediate P wave state.

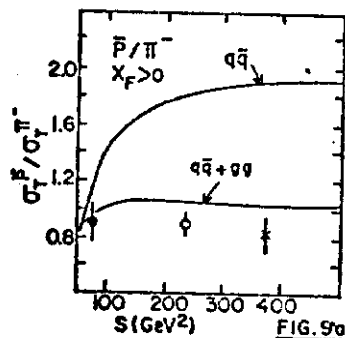


FIG. 9a

○ E537
• Ω
x NA3

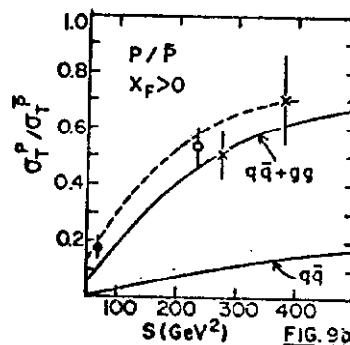


FIG. 9b

CERN experiment WA11 has attempted to determine the gluon structure function of the pion by analyzing J/ψ production in their 190 GeV/c π^- data. In performing this analysis they allowed for a 30.5% production of J/ψ by the direct production of a χ state which subsequently decays into a J/ψ plus a photon. This corrected X distribution which is shown in Fig. 10 was fit by varying the input π^- and nucleon structure function to the gluon fusion model for J/ψ production. The results obtained for the pion and nucleon gluon structure functions are $g_{\pi}(x_1) \sim (1-x_1)^{1.9 \pm 0.3}$ and $g_N(x_2) = (1-x_2)^{5.5}$. Negligible changes in the pion exponent takes place when the CDHS parameterization is used for the nucleon.

The final new contribution to the conference was the report of NA3 of the detection of di- ψ production in their 150 GeV/c and 280 GeV/c π^-N data. Out of a sample of 1,359,000 ψ events accumulated at the two energies, a total of 13 events with two J/ψ 's have been found (6 at 150 GeV/c and 7 at 280 GeV/c). This yield corresponds to a ratio (after correction for the $\mu^+\mu^-$ branching ratio) of $\sigma_{\psi\psi}/\sigma_{\psi} = (3.0 \pm 1.0) \times 10^{-4}$ and cross sections, $\sigma_{\psi\psi} = 18 \pm 8$ picobarns at 150 GeV/c, 30 ± 10 picobarns at 280 GeV/c. The acceptances used to arrive at these cross sections were calculated using either an uncorrelated $\psi\psi$ production or a model which assumes that the ψ 's are decay products of B mesons. The error in the cross sections includes the uncertainty in this acceptance due to the uncertainty in the production process.

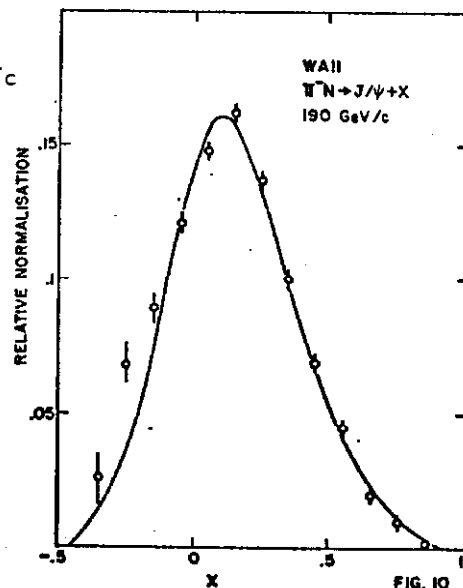
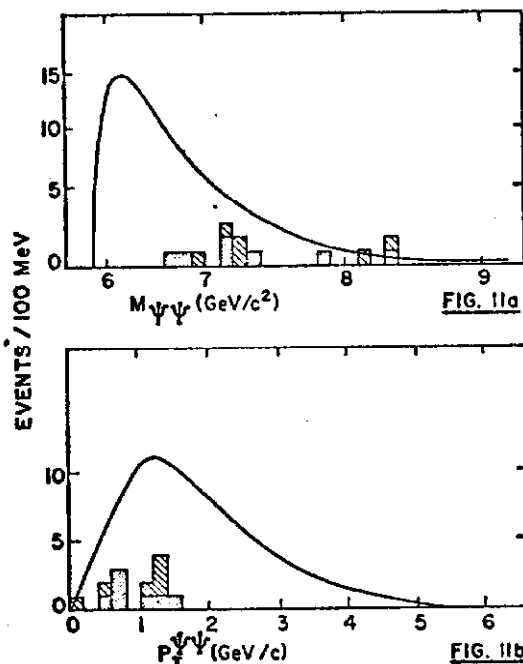


FIG. 10



The strong indication as seen in the mass spectrum of the di- ψ 's shown in Fig. 11a is that the ψ 's are correlated. The curve shown in this figure is the prediction for uncorrelated di- ψ 's. It peaks considerably below the average mass of the observed di- ψ events. (The cross hatched squares are the 150 GeV/c data.) A second evidence for a correlation between the two ψ 's is the p_T spectrum of the di- ψ system shown in Fig. 11b. The uncorrelated ψ model prediction peaks somewhat higher than the observed events. The experimenters have made no statement at this time about the production mechanism for the di- ψ 's because of the limited statistics.

Conclusion - Hadronic production of dimuons, both continuum and resonance, continues to be a rich source of information about the constituents of hadrons and their interactions. In particular with the present state of the continuum high mass data, quantum chromodynamics is beginning to be confronted with a wide variety of effects that the theory must explain. The first successes of low order QCD must now be followed with higher order calculations in order to explain the K factor and $\langle p_T \rangle$ behavior as a function of the various kinetic quantities. The resonance data on the other hand, while not having as complete theoretical framework for interpretation, is beginning to yield information about the gluon composition of the hadrons. In the future we can anticipate both new experiments and new analyses and perhaps new understandings of these fundamental processes.

REFERENCES

1. DRELL, S.D., and YAN, T.M., Phys. Rev. Letters 25, 316 (1970).
2. HALZEN, F., and SCOTT, D.H., Phys. Rev., D18 (1978), 3778.
3. ANASSONTZIS, E., et al., E-537 Collaboration, paper 665, XXI Int. Conf. on High Energy Physics, Paris, France, 1982/Fermilab Preprint, Conf-82/50-EXP, 7530.537.
4. BADIER, J., et al., NA3 Collaboration, Paper 350, XXI Int. Conf. on High Energy Physics, Paris, France, 1982/Ecole Polytechnique Preprint LPNE/X 82/02.
5. STICKLAND, D.P., et al., E-326 Collaboration, paper 169, XXI Int. Conf. on High Energy Physics, Paris, France, 1982.
6. ANASSONTZIS, E., et al., E-537 Collaboration, paper 656, XXI Int. Conf. on High Energy Physics, Paris, France, 1982/Fermilab Preprint, Conf-82/49-EXP, 7550.537.
7. PIETRZKY, B., et al., WA11 Collaboration, paper 625, XXI Int. Conf. on High Energy Physics, Paris, France, 1982.
8. BADIER, J., NA3 Collaboration, paper 535, XXI Int. Conf. on High Energy Physics, Paris, France, 1982/CERN Preprint, CERN-EP/82-67.
9. DE GROOT, J.G.H., et al., CDHS Collaboration, Phys. Letters 82B, 456 (1979).
10. ALTERELLI, et al., Physics Letters, 76B, 356 (1978).
11. ITO, A.S., et al., Phys. Rev. D23, 604 (1981).
12. BARGER, V., et al., Zeitschrift fur Physik C, 6, 169 (1980).
13. CARLSON, C.E., and SUAYA, R., Phys. Rev. 18D, 760 (1978).